Catalysis Science & Technology

Catalytic Oxidation of Methane to Methanol over Cu-CHA with Molecular Oxygen

Journal:	*Catalysis Science & Technology*
Manuscript ID	CY-ART-04-2021-000676.R1
Article Type:	Paper
Date Submitted by the Author:	18-Jun-2021
Complete List of Authors:	Hirayama, Airi; Kumamoto University, Graduate School of Science and Technology Tsuchimura, Yuka; Kumamoto University, Graduate School of Science and Technology Yoshida, Hiroshi; Kumamoto Daigaku, Machida, Masato; Kumamoto University, Applied Chemistry and Biochemistry Nishimura, Shun; Japan Advanced Institute of Science and Technology, Graduate School of Advanced Science and Technology Kato, Kazuo; Japan Synchrotron Radiation Research Institute, Takahashi, Keisuke; Hokkaido University, Department of Chemistry; National Institute for Materials Science, Center for Materials research by Information Ohyama, Junya; Kumamoto University, Faculty of Advanced Science and Technology

ARTICLE

Catalytic Oxidation of Methane to Methanol over Cu-CHA with Molecular Oxygen

Received 00th January 20xx,
Accepted 00th January 20xx

DOI: 10.1039/x0xx00000x

Airi Hirayama,[a] Yuka Tsuchimura,[a] Hiroshi Yoshida,[b] Masato Machida,[b] Shun Nishimura,[c] Kazuo Kato,[d] Keisuke Takahashi[e] and Junya Ohyama*[b]

Direct oxidation of CH_4 to CH_3OH using O_2 is challenging because of the high stability of CH_4 and the relatively high reactivity of CH_3OH. Here, Cu-CHA zeolites are tested for direct oxidation of CH_4. Catalytic production of CH_3OH in a CH_4-O_2-H_2O flow reaction is improved using CHA type zeolites compared to other zeolites including MOR, BEA, MFI, and FAU zeolites reported previously. In situ X-ray absorption fine structure (XAFS) spectroscopy reveals that high catalytic activity of Cu-CHA is derived from its redox property, particularly, the high reducibility of Cu^{2+} involved in CH_4 activation. The reaction gas concentrations are varied to find optimized reaction conditions on Cu-CHA. In addition, the reaction mechanism of the direct CH_4 oxidation on a Cu-CHA is investigated based on not only the effects of gas concentrations but also the isotope gas effects using CD_4, $^{18}O_2$, and D_2O. It is suggested that the rate-determining step is C-H activation of CH_4, and the selectivity of CH_3OH is determined by oxidation rate of CH_3OH, which is affected by O_2 and OH groups activation rate on Cu-CHA.

Introduction

Methanol (CH_3OH) production is growing as CH_3OH is increasingly used as chemical and fuel in the industry. In the current industrial process of CH_3OH production from natural gas, CH_3OH is produced via two steps, CH_4 steam reforming and CO hydrogenation, where high-temperature and high-pressure conditions are required.[1, 2] Therefore, direct synthesis of CH_3OH by CH_4 oxidation at low temperatures has attracted attention, because it can significantly reduce energy and cost for CH_3OH production.[2, 3] However, direct oxidation of CH_4 to CH_3OH is challenging because of the high stability of CH_4 and the relatively high reactivity of CH_3OH.[4, 5] Since the bond dissociation enthalpy of the C-H bond of CH_4 is about 46 kJ mol^{-1} higher than that of CH_3OH, it is difficult for CH_3OH to exist stably under CH_4 activation conditions.[4, 5] Thus, even if CH_3OH is formed, CH_3OH suffers from oxidation to CO and CO_2 under CH_4 oxidation conditions. Consequently, the trade-off between CH_4 conversion rate and CH_3OH selectivity can be a significant problem in the direct oxidation of CH_4 to CH_3OH.

It is known that methanotrophic bacteria in nature use metalloenzymes called methane monooxygenase (MMO) to achieve the direct oxidation of CH_4 under ambient conditions.[6] The structures of active centers in MMO have inspired researchers to design and develop artificial catalysts for the direct oxidation of CH_4.[7-9] Among the catalyst materials, metal exchanged zeolites, particularly, Cu zeolites have been attracted attentions because they form similar structures of Cu active sites to a soluble MMO (sMMO).[7-10] In fact, recent studies have revealed that Cu zeolites offer the direct oxidation of CH_4 to CH_3OH not only using relatively highly reactive oxidants such as H_2O_2 and NOx, but also using O_2.[11-17]

The direct oxidation of CH_4 to CH_3OH using O_2 has been achieved by chemical looping process over Cu zeolites, where Cu zeolites do not act as catalysts but stoichiometric oxidants for CH_4.[18, 19] The chemical looping process offers selective production of CH_3OH. However, the production rate is low and does not meet the criteria for practical application, because the looping process needs abstraction of CH_3OH by H_2O after CH_4 activation and then reactivation of Cu zeolites under O_2.[3, 18] To solve the complexity of the looping process and the low productivity of CH_3OH, continuous synthesis of CH_3OH by catalytic partial oxidation of CH_4 has been developed using Cu zeolites.[15-17] As a result, several Cu zeolites have been found to show catalytic activity for selective and continuous CH_3OH production at low temperatures, e.g. < 270 ^{O}C, and low O_2 concentrations, e.g., < 0.1%. However, the CH_3OH production is still low. Therefore, further development of catalysts with understanding of reaction mechanisms are necessary for improvement of the catalytic direct oxidation of CH_4 to CH_3OH.

In the previous study of the authors' research group, various Cu zeolites including Cu-MOR, Cu-BEA, Cu-MFI, and Cu-FAU have been tested for the direct oxidation of CH_4 at higher O_2

[a] Department of Applied Chemistry and Biochemistry, Graduate School of Science and Technology, Kumamoto University, 2-39-1 Kurokami, Chuo-ku, Kumamoto, 860-8555, Japan.
[b] Faculty of Advanced Science and Technology, Kumamoto University, 2-39-1 Kurokami, Chuo-ku, Kumamoto, 860-8555, Japan.
[c] Graduate School of Advanced Science and Technology, Japan Advanced Institute of Science and Technology (JAIST), 1-1 Asahidai, Nomi, 923-1292, Japan.
[d] Japan Synchrotron Radiation Research Institute, 1-1-1 Kouto, Sayo-cho, Sayo-gun, Hyogo, 679-5198, Japan
[e] Department of Chemistry, Hokkaido University, N-15 W-8, Sapporo, 060-0815, Japan.

† Electronic Supplementary Information (ESI) available: a reactor diagram; reaction schemes for kinetic isotope effect experiments; results of mass analysis. See DOI: 10.1039/x0xx00000x

concentration, e.g., 2 %, and higher temperature, e.g., 300 °C compared to the conditions of the other research groups' studies.[15-17] As a result, the CH_3OH production was greatly improved using Cu-MOR, although the CH_3OH selectivity was decreased to 30% with production of CO and CO_2. The more important finding is that the catalytic performance is largely varied with the catalysts and the reaction conditions. It is suggested that further exploration of Cu zeolites and reaction conditions can improve the direct oxidation of CH_4 to CH_3OH. Herein, Cu-CHA catalysts are tested for the direct oxidation of CH_4. The reason for the improved catalytic activity of Cu-CHA is investigated using in situ XAFS spectroscopy. In addition, the reaction mechanism of the direct CH_4 oxidation is investigated based on the variation of reaction kinetics with gas concentrations and isotope gases.

Experimental

Catalyst preparation

Cu(X)-CHA(Y) catalysts, where (X) is the Cu loading and (Y) is the Si/Al ratio, were prepared by an ion-exchange method. CHA zeolites were CHA5 and CHA10, supplied from JGC Catalysts and Chemicals Ltd. Ammonium exchanged CHA zeolite powder (2 g) was added to $Cu(CH_3COO)_2 \cdot H_2O$ aqueous solution (200 mL) and stirred at 80 °C for 3 h . The suspension was then filtered and washed with water. In the case of the preparation of Cu2.8-CHA10, the ion exchange process was performed twice at room temperature. After the ion exchange, the catalysts were dried at 110 °C and then calcined at 700 °C for 1 h.

Catalytic reaction

CH_4-O_2-H_2O reaction was carried out using a fixed-bed reactor, where 50 mg of catalyst was placed in a quartz glass tube with an inner diameter of 4 mm (Figure S1). The catalyst was pretreated at 550 °C for 30 min under 15 mL min^{-1} of O_2. After cooling to 300 °C, the reaction tube was purged with 50 mL min^{-1} of N_2 for 30 min, and then the reaction gas composed of CH_4, O_2, N_2, and H_2O(g) was flown at 110 mL min^{-1} to the catalyst bed. H_2O(g) was supplied using a vapor mixing system (Bronkhorst μ-FLOW L01 and CEM W-101A). The outlet gas was cooled by a cold trap at 10 °C. The trapped aqueous solution was analyzed by high performance liquid chromatography (HPLC, JASCO LC-200 Plus) equipped with a Shodex RSpak DE-413L column (Showa Denko) and refractive index (RI) and UV detectors. The amount of CH_3OH in the trapped solution was corrected by evaporated amounts evaluated using Raoult's law and CH_3OH vapor pressure of 569.2 Pa at 9.96 °C. The amount of HCHO was as detected without correction of evaporation, because most of the HCHO in the trapped aqueous solution is assumed hydrated to form methanediol and its evaporation is negligible. The gas phase components were analyzed by a GC (Shimadzu GC-2014) equipped with a thermal conductivity detector (TCD) and a Shincarbon ST column (Shinwa Chemical Industries LTD.), one equipped with a flame ionization detector (FID) and a HP-PLOT Q column (Agilent) after a methanizer (Shimadzu MTN-1), and a quadrupole mass (QMS) analyzer (BELMASS, MicrotracBEL Corp.). The isotope effect experiments were performed using CD_4 (99%, Cambridge Isotope Laboratories, Inc.), $^{18}O_2$ (98%, Shoko Science Co., Ltd.), and D_2O (99.8%, FUJIFILM Wako Pure Chemical Co.) instead of CH_4 (99.9%, TAIYO NIPPON SANSO Co.), O_2 (>99.5%, TAIYO NIPPON SANSO Co.), and H_2O (Milli-Q), respectively. The production rates during the isotope effect experiments were evaluated from the reaction under every gas condition for 2.5 h as shown in Schemes S1. Only in the isotope effect experiment of H_2O/D_2O, bubblers at 47 ºC were used to switch between H_2O and D_2O with ca. 0.5 g h^{-1} of flow rate instead of the vapor mixing system used in the other experiments.

Characterization

The X-ray fluorescence (XRF) intensity of Cu-CHA zeolites was evaluated by an energy dispersive XRF analyzer (Rigaku EDXL 300). The Cu content was determined from the previously reported linear relationship between the XRF intensity of Cu / (Cu + Al + Si) and the Cu contents determined by an inductivity coupled plasma optical emission spectrometer.[11]

In situ XAFS measurement

The in situ XAFS measurement was performed at BL01B1 at SPring-8. A sample in pellet form (ϕ 7 mm, 34 mg of Cu2.5-CHA10 or 48 mg of Cu2.0-MOR10) was set to an in situ cell, where gas can flow through the sample under heat. Cu K-edged XAFS spectra were taken in a transmission mode. The sample was pretreated at 550 °C for 30 min under 50 mL min^{-1} of O_2. The sample was cooled to 300 °C, then the cell was purged with 50 mL min^{-1} of He, where a XAFS spectrum after the pretreatment was taken. After a wet He gas flow (He 50 mL min^{-1} + H_2O(g) 0.5 g h^{-1}), the following gases were flown in the order: a reaction gas (CH_4 48 mL min^{-1} + O_2 2mL min^{-1} + He 50 mL min^{-1} + H_2O(g) 0.5 g h^{-1}); a reduction gas (CH_4 48 mL min^{-1} + He 52 mL min^{-1} + H_2O(g) 0.5 g h^{-1}); a oxidation gas (O_2 2mL min^{-1} + He 98 mL min^{-1} + H_2O(g) 0.5 g h^{-1}); and the reduction gas again. H_2O(g) was supplied using a water babbler controlled at 48°C. During the gas flow variation, XAFS spectra were obtained. The XAFS data were analyzed using Athena software in Demeter package.

Results and discussion

Catalytic activity

Figure 1 show the time course of CH_3OH, CO, and CO_2 production in a CH_4-O_2-H_2O reaction at 300 °C over Cu2.5-CHA10, Cu2.8-CHA10, Cu4.1-CHA5, and Cu3.4-CHA5, where CH_3OH, CO and CO_2 were continuously detected over all Cu-CHA catalysts for at least 24 h while they were not significantly decreased. The CH_3OH production was confirmed by HPLC analysis of the liquid trapped after the reaction. In addition, HCHO was detected in the trapped solution, although formic acid was not detected. The accumulated amount of the products for the 24 h reaction over Cu-CHA were presented in Figure 2. It should be noted that the amounts of CH_3OH evaluated by GC-FID contains some errors (ca. 20% underestimation) because of overlap of broad peaks derived from HCHO on the peaks of CH_3OH. Thus, the amounts of CH_3OH

in Figure 2 are the ones evaluated by HPLC with correction of evaporated amounts based on Raoult's law. More importantly, the product distributions are changed by the Cu-CHA catalysts. Table 1 entry 1 – 4 shows the product yields, the CH_3OH production rates, the turnover numbers (TON), and the selectivity of the four types of Cu-CHA under identical reaction conditions. Among the catalysts, Cu2.5-CHA10 produced the largest amount of CH_3OH, which was 8.8 $mmol_{CH3OH}$ g_{cat}^{-1} with the average production rate of 6.1 μmol_{CH3OH} g_{cat}^{-1} min^{-1}. The CH_4 conversion of Cu2.5-CHA10 was 0.06%, and the selectivity for only CH_3OH and on for the total of CH_3OH and HCHO were 22% and 41%, respectively. Although the CH_3OH yield was decreased from that of Cu2.5-CHA10, Cu3.4-CHA5 produced CH_3OH and HCHO with relatively high selectivity, 63% and 87 % in terms of the production of only CH_3OH and the total of CH_3OH and HCHO, respectively. One can find that CHA5 offers higher selectivity than CHA10. High Al content in CHA, i.e., large amount or high density of ion exchange sites, might contribute to the improved selectivity. The TONs of Cu-CHA based on the amount of CH_3OH (TON_{CH3OH}) were greater than 10 mol_{CH3OH}/mol_{Cu}. In addition, those based on the total of CH_3OH and HCHO ($TON_{CH3OH+HCHO}$) were more than 20 $mol_{CH3OH+HCHO}/mol_{Cu}$. The TONs confirm that all the Cu-CHA act as catalysts for the CH_4 partial oxidation, not as simple oxidant for CH_4 oxidation.

In the previous study of the authors' research group, the other types of Cu zeolites including Cu-MOR, Cu-BEA, Cu-MFI, and Cu-FAU were tested for the CH_4-O_2-H_2O reaction under the same reaction conditions as Cu-CHA in the entry 1-4 of Table 1.[15] Among the other zeolites, Cu2.0-MOR10 showed the largest TON_{CH3OH} and $TON_{CH3OH+HCHO}$, which were 7.4 and 10.9, respectively, as shown in entry 5 of Table 1. Compared to Cu2.0-MOR10, Cu2.5-CHA10 exhibits ca. 3 – 4 times larger TONs, but lower selectivity of CH_3OH and HCHO. However, Cu3.4-CHA5 presents about twice higher TONs with much higher selectivity. Therefore, CH_3OH and HCHO production over Cu-zeolite is improved by using CHA type zeolites.

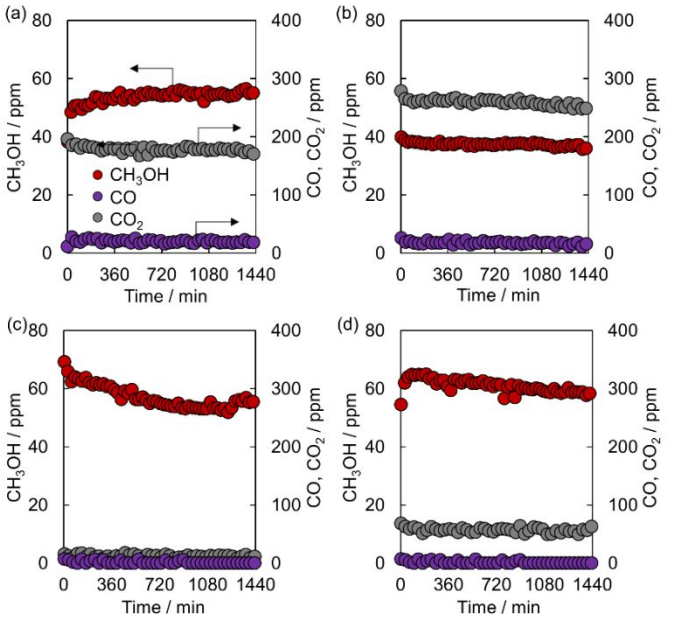

Figure 1. Time course of CH_3OH (red), CO (purple), and CO_2 (gray) production in the CH_4-O_2-H_2O reaction over (a) Cu2.5-CHA10, (b) Cu2.8-CHA10, (c) Cu4.1-CHA5, and (d) Cu3.4-CHA5. Reaction conditions: catalyst 50 mg, 300 °C, CH_4 (48 mL min^{-1}) + O_2 (2 mL min^{-1}) + N_2 (50 mL min^{-1}) + H_2O(g) (0.5 g h^{-1}).

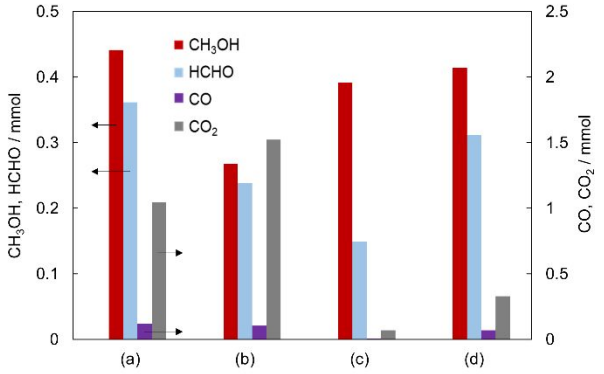

Figure 2. Product amounts of CH_4-O_2-H_2O reaction for 24 h over (a) Cu2.5-CHA10, (b) Cu2.8-CHA10, (c) Cu4.1-CHA5, and (d) Cu3.4-CHA5. Reaction conditions: catalyst 50 mg, 300 °C, CH_4 (48 mL min^{-1}) + O_2 (2 mL min^{-1}) + N_2 (50 mL min^{-1}) + H_2O(g) (0.5 g h^{-1}). CH_3OH and HCHO were evaluated by HPLC. CO and CO_2 were evaluated by GC-TCD.

ARTICLE

Table 1. Results of CH_4-O_2-H_2O reaction for 24 h over Cu-CHA together with those over Cu2.0-MOR10 for comparison.

Entry	Catalyst	CH_3OH yield [a] ($mmol_{CH3OH}$ g_{cat}^{-1})	CH_3OH production rate [b] (μmol_{CH3OH} g_{cat}^{-1} min^{-1})	HCHO yield [a] ($mmol_{HCHO}$ g_{cat}^{-1})	CO_2 yield [c] ($mmol_{CO2}$ g_{cat}^{-1})	CO yield [c] ($mmol_{CO}$ g_{cat}^{-1})	TON for CH_3OH (mol_{CH3OH}/mol_{Cu})	TON for CH_3OH + HCHO ($mol_{CH3OH+HCHO}$/mol_{Cu})	TON for all products ($mol_{CH3OH+HCHO+CO+CO2}$/mol_{Cu})	CH_3OH selectivity (%)	CH_3OH + HCHO selectivity (%)	CH_4 conversion (%)
1[d]	Cu2.5-CHA10	8.8	6.1	7.2	20.7	2.4	22.3	40.5	99.2	22	41	0.06
2[d]	Cu2.8-CHA10	5.3	3.7	4.7	30.2	2.0	12.1	22.8	96.0	13	24	0.07
3[d]	Cu3.4-CHA5	7.8	5.4	3.0	1.4	0.1	14.5	20.1	22.9	63	87	0.02
4[d]	Cu4.1-CHA5	8.2	5.7	6.1	6.5	1.4	12.7	22.2	34.4	37	65	0.04
5[d,e]	Cu2.0-MOR10	2.3	1.6	1.1	3.2	0.0	7.4	10.9	21	34	52	0.011
6[f]	Cu2.5-CHA10	16.3	11.3	5.8	13.4	1.9	41	56	92	45	60	0.06

[a] Obtained by 24 h reaction and evaluated by HPLC. [b] Averaged over 24 h. [c] Obtained by 24 h reaction and evaluated by GC-TCD. [d] Reaction results under CH_4 (48 mL min^{-1}) + O_2 (2 mL min^{-1}) + N_2 (50 mL min^{-1}) + H_2O(g) (0.5 g h^{-1}). [e] Previously reported data in ref. 15. [f] Reaction results under CH_4 (78 mL min^{-1}) + O_2 (1 mL min^{-1}) + H_2O(g) (1.5 g h^{-1}) for 2.5 h. The presented data for 24 h reaction were calculated from the results of the reaction for 2.5 h.

Redox of Cu species

Since the previous study has suggested that the redox of Cu species in zeolites is the key for the catalytic activity for CH_4 oxidation, the redox of Cu2.5-CHA10 was evaluated and compared to that of Cu2.0-MOR10 in order to reveal the reason for the high catalytic activity of Cu-CHA catalysts. The redox of Cu species was observed using the in situ XAFS spectroscopy. Figure 3(a) shows the Cu K-edge X-ray absorption near edge structure (XANES) spectra of Cu2.5-CHA10 after the pretreatment, the reaction gas, the reduction gas and the oxidation gas flows. The spectra were obtained after almost no change was observed under each gas flow. The spectrum after the pretreatment exhibited the feature of dehydrated Cu^{2+} species with shoulder peak at 8988 eV. The reaction gas flow caused a spectral change, and increased the shoulder peak at 8985 eV, which is assignable to the 1s to 4p transition of Cu^+ species. The reduction gas flow further changed the spectrum to show the peak due to Cu^+ species more prominently. Accordingly, the reaction and reduction gas flows caused reduction of Cu^{2+} to Cu^+. Then, the oxidation gas flow decreased the shoulder peak and the spectral feature returned to that of Cu^{2+} species. Thus, Cu^+ was oxidized to Cu^{2+} by the oxidation gas flow. It should be noted that the spectrum under the reaction gas flow exhibits an intermediate feature of those under the reduction and oxidation gas flows. The Cu species are considered in the middle of the redox under the reaction conditions. Similar spectral change was also observed on Cu2.0-MOR10 (Figure 3(b)). However, the magnitude of the change, more specifically, the peak intensity due to the Cu^+ formation was different between the catalysts, and Cu2.5-CHA10 exhibited larger spectral change than Cu2.0-MOR10. It is suggested that Cu2.5-CHA10 has more Cu species that are redox active in the reaction conditions. Since the reaction proceeds with the redox of Cu species, Cu2.5-CHA10 has more active Cu species for the CH_4 oxidation reaction than Cu2.0-MOR10. This can explain the enhanced catalytic activity of Cu-CHA zeolites.

For further investigation of the reason for the enhanced catalytic activity of Cu-CHA zeolites, the redox rates were evaluated from the variation of in situ XANES spectra. Figure 4 shows the Initial change of the absorbance at 8985 eV ($\boldsymbol{A}_{8985}$) of Cu2.5-CHA10 and Cu2.0-MOR10 at the oxidation gas flow to the reduced samples (a) and at the reduction gas flow to the oxidized samples (b). The decrease and increase of $\boldsymbol{A}_{8985}$ indicate the reduction and oxidation of Cu species, respectively. When the initial change rates of $\boldsymbol{A}_{8985}$ were compared between the oxidation step (Figure 4(a)) and the reduction step (Figure 4(b)), the rate in the reduction step was lower on both catalysts. This suggests that the reduction step is involved in the rate determining step of the catalytic CH_4 oxidation reaction. In other words, the CH_4 activation with the reduction of Cu^{2+} is the rate determining step. It was found that Cu2.5-CHA10 showed

faster change of A_{8985} in the reduction step than Cu2.0-MOR10 (Figure 4(b)). This means that the reduction of Cu2.5-CHA10 is faster than that of Cu2.0-MOR10. Therefore, the high catalytic activity of Cu-CHA zeolites can be explained by the increase of reactive Cu species and their improved reduction rate, or in other words, CH_4 activation.

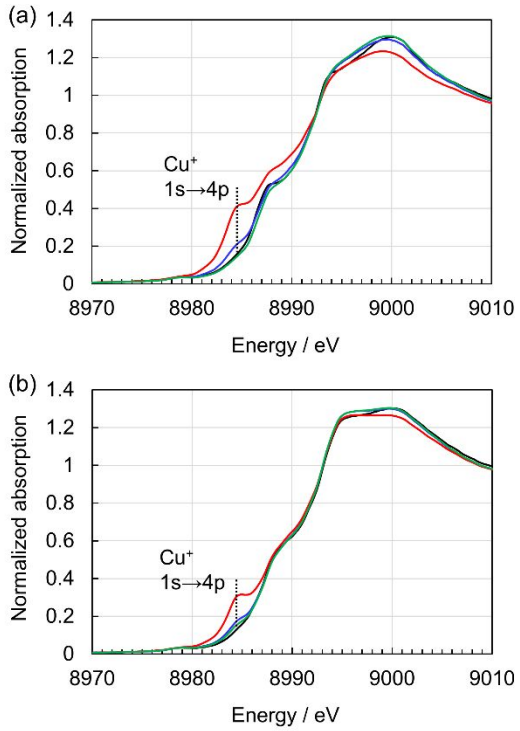

Figure 3. Cu K-edge XANES spectra of (a) Cu2.5-CHA10 and (b) Cu2.0-MOR10 after the pretreatment (black), the reaction gas (blue), the reduction gas (red) and the oxidation gas (green) flows.

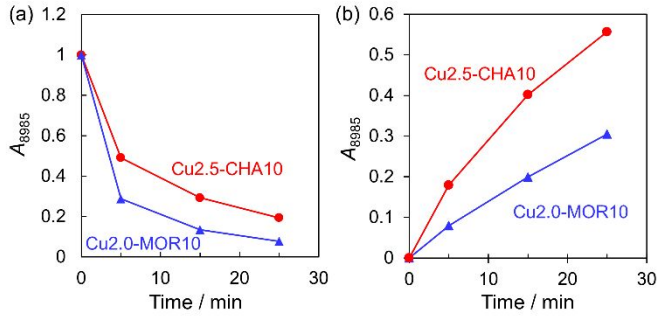

Figure 4. Initial change of A_{8985} of Cu2.5-CHA10 and Cu2.0-MOR10 at the oxidation gas flow to the reduced samples (a) and at the reduction gas flow to the oxidized samples (b).

Effects of reaction gas concentrations

The effects of reaction gas concentrations were investigated by conducting CH_4-O_2-H_2O reaction using Cu2.5-CHA10 at the total gas flow rate of 110 mL min^{-1}. Figure 5(a) shows the effect of CH_4 concentration on the product yields. As the CH_4 concentration increased, all the oxidized products increased; however, the response to the change of CH_4 concentration was different between the products. The amounts of CH_3OH, HCHO, and CO were increased more sharply than that of CO_2, indicating that the increase of CH_4 concentration can improve both the yield and the selectivity of partial oxidation products.

The effect of O_2 concentration is presented in Figure 5(b). Without O_2 flow, almost no products were obtained, suggesting that O_2 plays a major role as an oxidant in CH_4-O_2-H_2O reactions. The increase of O_2 concentration to 1% caused production of all compounds. However, CH_3OH decreased by further increase of O_2 to > 1% and also HCHO decreased by increasing O_2 to > 2%. In contrast, CO and CO_2 rose with the O_2 concentration. In addition, the increased amount of CO_2 is much larger than the decreased amount of CH_3OH and HCHO. Thus, the effect of O_2 is more prominent on CO_2 production than on the partial oxidation products. It is suggested that tuning of O_2 concentration is important for improvement of both the yield and the selectivity of CH_3OH.

The effect of H_2O concentration at 0 – 40% is shown in Figure 5(c). CH_3OH increased at > 2% H_2O, and CO simply decreased with the H_2O concentration. Meanwhile, HCHO increased slightly with the H_2O concentration at 0 – 5%, then decreased. The CO_2 production also exhibited a volcano dependence with a peak at 2% H_2O. The H_2O concentration dependence suggests that H_2O is effective for promoting desorption of CH_3OH before it suffers from overoxidation. Therefore, in the range of H_2O concentration tested, the higher the H_2O concentration, the larger the yield of CH_3OH produced.

Based on the results, in the case of CH_4-O_2-H_2O reaction using Cu2.5-CHA10, the CH_3OH yield and selectivity can be optimized by increase of CH_4 or H_2O concentration and control of O_2 concentration to < ca. 2%. In fact, the reaction was performed under CH_4 78 mL min^{-1}/O_2 1 mL min^{-1}/H_2O(g) 31 mL min^{-1} (1 g h^{-1}) using Cu2.5-CHA10. The reaction result is presented in entry 6 of Table 1. The CH_3OH yield and selectivity are improved by the optimization (cf. Table 1 entry 1). Therefore, the partial oxidation of CH_4 over Cu-CHA was improved by optimization of the reaction conditions based on understanding of the effects of each reaction gas concentration.

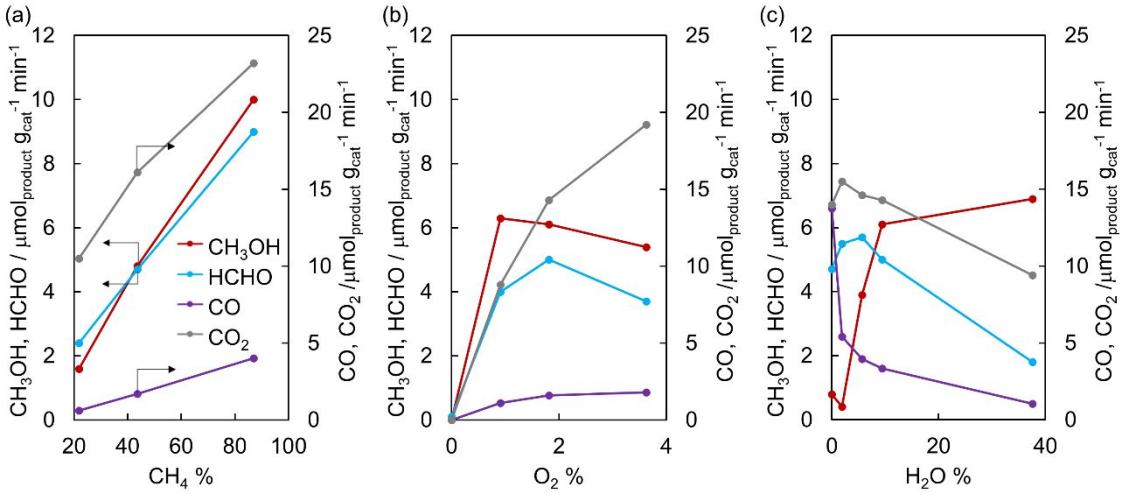

Figure 5. Production rate of CH_3OH (red, left axis), HCHO (blue, left axis), CO (purple, right axis), and CO_2 (gray, right axis) under various concentrations of (a) CH_4, (b) O_2, and (c) H_2O over Cu2.5-CHA10. The total gas flow rate was kept at 110 mL min^{-1} during the variation of reactant gas concentrations by changing N_2 flow rate.

Isotope effects

The isotope effects of the reactants were evaluated on a CH_4-O_2-H_2O reaction over Cu2.5-CHA10 in order to investigate the reaction kinetics and mechanism. First, the isotope effect of CH_4 was evaluated by changing the gas flow from CH_4-O_2-H_2O to CD_4-O_2-H_2O and backing to CH_4-O_2-H_2O at identical concentrations of the reactants (Scheme S1(a)). Before changing the gas flow, the reactants and the products were purged with N_2-H_2O. The product yields under each gas flow are presented in Figure 6(a). It is found that all the products are largely reduced by flowing CD_4 as the reactant. In addition, the formation of CD_3OH under CD_4-O_2-H_2O reaction was confirmed by QMS analysis as presented in Figure S2. The kinetic isotope effect of CH_4 (KIE_{CH4}) was evaluated from the ratio of the production rates of the total products under the first CH_4-O_2-H_2O flow to that of under the CD_4-O_2-H_2O flow. As a result, the KIE_{CH4} value was 2.2, which is significantly greater than 1. It is suggested that the C-H cleavage of CH_4 is the rate determining step of CH_4-O_2-H_2O reaction. The result is consistent with that of in situ XAFS analysis. Therefore, the C-H activation accompanied with the reduction of Cu^{2+} species is the rate determining step of the reaction.

The isotope effect of O_2 was also evaluated by switching the gas flow from CH_4-$^{16}O_2$-H_2O to CH_4-$^{18}O_2$-H_2O and to CH_4-$^{16}O_2$-H_2O at the same concentration of the reactants (Scheme S1(b)). The amounts of products under each gas flow are shown in Figure 6(c). The KIE of O_2 (KIE_{O2}) was evaluated from the ratio of the production rate of the total products under the CH_4-$^{16}O_2$-H_2O flow to that under the CH_4-$^{18}O_2$-H_2O flow. The KIE_{O2} value was 1.0, indicating that O_2 involved reactions do not determine the overall reaction rate. Interestingly, however, the product distribution was changed by using $^{18}O_2$. The amount of CH_3OH rose by changing the gas from CH_4-$^{16}O_2$-H_2O to CH_4-$^{18}O_2$-H_2O. In contrast, the amount of CO_2 diminished by changing the gas flow from CH_4-$^{16}O_2$-H_2O to CH_4-$^{18}O_2$-H_2O, and was increased again by returning to CH_4-$^{16}O_2$-H_2O. The same behavior as the CO_2 production was observed in the HCHO and CO production. This behavior can be explained by change in the relative rate of the overoxidation to the production rate of CH_3OH, which is lowered under $^{18}O_2$ to increase CH_3OH and decrease the overoxidized products. The result is consistent with the effect of O_2 concentration (Figure 2(b)), where the lower the O_2 concentration, the higher the CH_3OH production and the lower the overoxidation products, although the reaction without O_2 could hardly offer any oxidized products. Therefore, O_2 is not involved in the rate determining step of CH_4 oxidation over Cu2.5-CHA10, but in the step of CH_3OH oxidation. According to the literature, the oxidation of CH_3OH is considered initiated by formation of methoxide intermediate on the catalyst surface, and then the C-H of methoxide is activated to form the overoxidized products.[20] Thus, one can consider that O_2 activation on the Cu-CHA might be slow or comparable for the activation steps of CH_3OH, although it is fast enough for the activation of CH_4. Therefore, the isotope effects of O_2 on the product distribution can be explained by contribution of O_2 activation to CH_3OH oxidation.

To investigate the KIE of H_2O (KIE_{H2O}), the reaction gas flow was changed between CH_4-O_2-H_2O and CH_4-O_2-D_2O. Figure 6(b) shows the product amounts under the gas flows containing H_2O and D_2O. It should also be noted that the amount of HCHO in the CH_4-O_2-D_2O reaction was not able to be evaluated by HPLC with a RI detector due to overlap of signal from D_2O in the analysis conditions of this study. Thus, the KIE_{H2O} value was estimated from the ratio of the production rates of the total products other than HCHO, which was 1.0. It is suggested that H_2O is not involved in the rate determining step. However, the change of H_2O to D_2O caused variation of product distribution, slight increase of $CH_3OH(D)$ yield and slight decrease of CO_2 yield. In other words, the oxidation of CH_3OD became slower than that of CH_3OH. D_2O can exchange OH groups of CH_3OH and on catalyst surface to OD groups. Thus, the isotope effect of D_2O suggests that the activation of $OH(D)$ groups of $H(D)_2O$,

CH_3OH(D) and/or catalyst surface contribute to the reaction kinetics for oxidation of CH_3OH(D). In other words, the OH(D) activation step(s) are considered slow, comparable to the C-H activation of methoxide.

As above, the reaction mechanism of CH_4 partial oxidation over Cu-CHA has been revealed by the investigation of the isotope effects. The rate-determining step is C-H activation, which is supported by the results of the in situ XAFS analysis. In addition, the product distribution, more specifically, the selectivity of CH_3OH is determined by its oxidation rate affected by the O_2 activation and/or the OH activation on Cu-CHA.

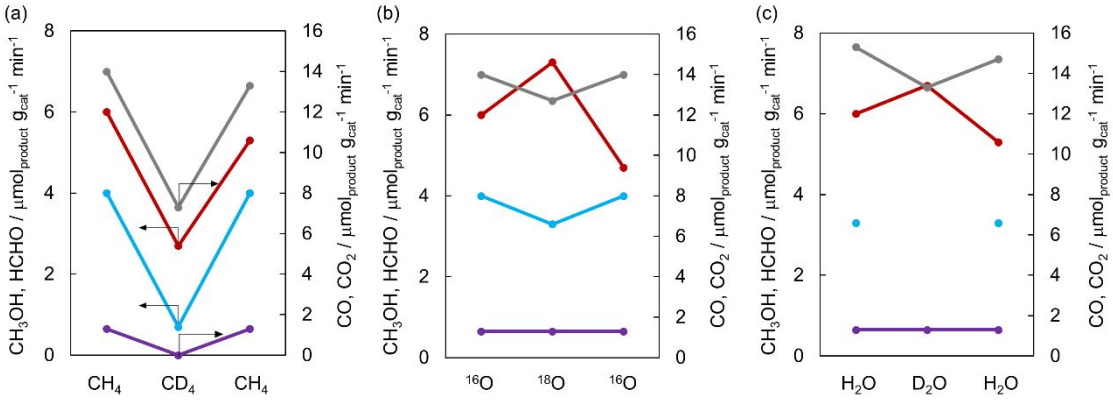

Figure 6. Variation of production rates of methanol (CH_3OH, CD_3OH, or $CH_3{}^{18}OH$, red, left axis), formaldehyde (HCHO or $HCH^{18}O$, blue, left axis), carbon monoxide (CO or $C^{18}O$, purple, right axis), and carbon dioxide (CO_2, $CO^{18}O$, or $C^{18}O_2$, gray, right axis) under (a) CH_4/CD_4-O_2-H_2O, (b) CH_4-$^{16}O_2/^{18}O_2$-H_2O, and (c) CH_4-O_2-H_2O/D_2O reaction over Cu2.5-CHA10. Reaction conditions: catalyst 50 mg, 300 °C, CH_4/CD_4 (48 mL min^{-1}) + $^{16}O_2/^{18}O_2$ (2 mL min^{-1}) + N_2 (50 mL min^{-1}) + H_2O/D_2O(g) (0.5 g h^{-1}). The experimental error evaluated by the standard deviation of the four data under the identical experimental conditions in Figure 6(a) and (b): 0.6, 0.0, 0.0 and 0.4 μmol g_{cat}^{-1} min^{-1} for CH_3OH, HCHO, CO and CO_2, respectively.

Conclusions

Cu-CHA zeolites showed catalytic activity for direct oxidation of CH_4 to CH_3OH in a CH_4-O_2-H_2O flow reaction at 300°C. The TON and the selectivity of CH_3OH were improved by Cu-CHA compared to the other Cu-zeolites including MOR, BEA, MFI, and FAU reported previously. The in situ XAFS analysis of Cu2.5-CHA10 and Cu2.0-MOR10 suggested that the increase of reactive Cu species and the improved reduction rate are responsible for the high catalytic performance of Cu-CHA catalysts. In addition, the catalytic performance of Cu-CHA was further improved by optimization of the reaction gas concentrations. More specifically, CH_3OH production rate and selectivity of Cu2.5-CHA10 were improved at relatively high concentrations of CH_4 (ca. 70%) and H_2O (ca. 30%) and low concentration of O_2 (ca. 1%). The reaction mechanism of the direct CH_4 oxidation on Cu2.5-CHA10 was investigated based on not only the effects of the reaction gas concentrations but also the isotope gas effects using CD_4, $^{18}O_2$, and D_2O. The results suggested that the rate-determining step is C-H activation of CH_4, and the CH_3OH selectivity is determined by oxidation rate of CH_3OH, which is affected by O_2 activation on Cu species and OH activation of H_2O, CH_3OH and/or catalyst surface.

Conflicts of interest

There are no conflicts to declare.

Acknowledgements

This work was funded in part by the Japan Science and Technology Agency (JST) CREST (JPMJCR17P2) and the Japan Society for the Promotion of Science (JSPS) KAKENHI through a Grant-in-Aid for Scientific Research (B) (20H02524). The in situ XAFS experiments were performed at the BL01B1 of Spring-8 with the approval of the Japan Synchrotron Radiation Research Institute (JASRI) (Proposal No. 2020A0534). The authors appreciate the JGC Catalysts and Chemicals Ltd., Japan, for their assistance in the CHA type zeolites.

Notes and references

1 E. V. Kondratenko, T. Peppel, D. Seeburg, V. A. Kondratenko, N. Kalevaru, A. Martin and S. Wohlrab, *Catal. Sci. Tech.*, 2017, **7**, 366-381.
2 V. L. Sushkevich, D. Palagin, M. Ranocchiari and J. A. van Bokhoven, *Science*, 2017, **356**, 523-527.
3 J.-P. Lange, V. L. Sushkevich, A. J. Knorpp and J. A. van Bokhoven, *Ind. Eng. Chem. Res*, 2019, **58**, 8674-8680.
4 N. J. Gunsalus, A. Koppaka, S. H. Park, S. M. Bischof, B. G. Hashiguchi and R. A. Periana, *Chem. Rev.*, 2017, **117**, 8521-8573.
5 R. Horn and R. Schlögl, *Catal. Lett.*, 2015, **145**, 23-39.
6 S. Sirajuddin and A. C. Rosenzweig, *Biochemistry*, 2015, **54**, 2283-2294.
7 M. H. Mahyuddin, Y. Shiota, A. Staykov and K. Yoshizawa, *Acc. Chem. Res.*, 2018, **51**, 2382-2390.
8 M. H. Mahyuddin, Y. Shiota and K. Yoshizawa, *Catal. Sci. Tech.*, 2019, **9**, 1744-1768.
9 B. E. R. Snyder, M. L. Bols, R. A. Schoonheydt, B. F. Sels and E. I. Solomon, *Chem. Rev.*, 2018, **118**, 2718-2768.
10 A. R. Kulkarni, Z.-J. Zhao, S. Siahrostami, J. K. Nørskov and F. Studt, *Catal. Sci. Tech.*, 2018, **8**, 114-123.
11 J. Ohyama, A. Hirayama, N. Kondou, H. Yoshida, M. Machida, S. Nishimura, K. Hirai, I. Miyazato and K. Takahashi, *Scientific Reports*, 2021, **11**, 10.

12 C. Hammond, M. M. Forde, M. H. Ab Rahim, A. Thetford, Q. He, R. L. Jenkins, N. Dimitratos, J. A. Lopez-Sanchez, N. F. Dummer, D. M. Murphy, A. F. Carley, S. H. Taylor, D. J. Willock, E. E. Stangland, J. Kang, H. Hagen, C. J. Kiely and G. J. Hutchings, *Angew. Chem. Int. Ed.*, 2012, **51**, 5129-5133.
13 P. Xiao, Y. Wang, T. Nishitoba, J. N. Kondo and T. Yokoi, *Chem. Commun.*, 2019, **55**, 2896-2899.
14 T. Sheppard, C. D. Hamill, A. Goguet, D. W. Rooney and J. M. Thompson, *Chem. Commun.*, 2014, **50**, 11053-11055.
15 J. Ohyama, A. Hirayama, Y. Tsuchimura, N. Kondou, H. Yoshida, M. Machida, S. Nishimura, K. Kato, I. Miyazato and K. Takahashi, *Catal. Sci. Tech.*, 2021, DOI: 10.1039/d1cy00125f, 10.
16 K. Narsimhan, K. Iyoki, K. Dinh and Y. Román-Leshkov, *ACS Cent. Sci.*, 2016, **2**, 424-429.
17 K. T. Dinh, M. M. Sullivan, K. Narsimhan, P. Serna, R. J. Meyer, M. Dincă and Y. Román-Leshkov, *J. Am. Chem. Soc.*, 2019, **141**, 11641-11650.
18 P. Tomkins, M. Ranocchiari and J. A. van Bokhoven, *Acc. Chem. Res.*, 2017, **50**, 418-425.
19 D. K. Pappas, E. Borfecchia, M. Dyballa, I. A. Pankin, K. A. Lomachenko, A. Martini, M. Signorile, S. Teketel, B. Arstad, G. Berlier, C. Lamberti, S. Bordiga, U. Olsbye, K. P. Lillerud, S. Svelle and P. Beato, *J. Am. Chem. Soc.*, 2017, **139**, 14961-14975.
20 H. Liu and E. Iglesia, *J. Phys. Chem. B*, 2005, **109**, 2155-2163.